

# Analysis of Thermal Conductivity, Surface Roughness, and Hardness of Carbon Nanotube-Reinforced Three-Dimensional Printed Acrylic Resin

**Ranin Raad Khalid<sup>1</sup>**  , **Abdalbseet A Fatalla<sup>\*1</sup>**  , **Matheel AL-Rawas<sup>2</sup>**  , **Yanti Johari<sup>2</sup>**   
, **Yew Hin Beh<sup>3</sup>**  , **Johari Yap Abdullah<sup>4,5</sup>**  

<sup>1</sup>Department of Prosthodontics, College of Dentistry, University of Baghdad, Baghdad, Iraq.

<sup>2</sup>Prosthodontic Unit, School of Dental Sciences, Universiti Sains Malaysia, Kubang Kerian, Malaysia.

<sup>3</sup>Department of Restorative Dentistry, Faculty of Dentistry, Universiti Kebangsaan Malaysia, Kuala Lumpur, Malaysia.

<sup>4</sup>Craniofacial Imaging Laboratory, School of Dental Sciences, Health Campus, Universiti Sains Malaysia, Kubang Kerian, Kota Bharu 16150, Malaysia

<sup>5</sup>Dental Research Unit, Center for Transdisciplinary Research (CFTR), Saveetha Dental College, Saveetha Institute of Medical and Technical Sciences, Saveetha University, Chennai 602105, India.

\*Corresponding Author.

Received 06/08/2024, Revised 20/10/2024, Accepted 22/10/2024, Published Online First 20/12/2024



© 2022 The Author(s). Published by College of Science for Women, University of Baghdad.

This is an open-access article distributed under the terms of the [Creative Commons Attribution 4.0 International License](https://creativecommons.org/licenses/by/4.0/), which permits unrestricted use, distribution, and reproduction in any medium, provided the original work is properly cited.

## Abstract

The dentistry field is in continuously developing, especially with three-dimensional (3D) printing technology. This study aims to analyze how resin 3D-printed denture bases affect the thermal conductivity, surface roughness, and surface hardness when carbon nanotubes (CNTs) are added at various weight percentages. 3D-printed denture base acrylic resin has been enhanced with CNTs. The samples were divided into three groups (0.5% and 0.7% of CNTs by weight, and a control group with no added CNTs). All samples underwent thermal conductivity, surface roughness, and surface hardness tests. In addition to conducting analyses using Fourier transforms, infrared spectroscopy, and field emission scanning electron microscopy, the data were analyzed using one-way analysis of variance (ANOVA) and multiple comparison tests. Incorporating CNTs into 3D-printed denture bases enhanced surface hardness, roughness, and heat conductivity compared to the control group. This improvement is directly correlated with the concentration of CNTs added. Integrating of CNTs enhances the material's mechanical properties, specifically its thermal conductivity and surface hardness. However, it does not have a great impact on surface roughness. Therefore, caution must be taken when selecting the appropriate CNTs concentrations to be added to the 3D-printing resin to improve the material characteristics.

**Keywords:** 3D printing, Carbon nanotubes, Digital dentistry, Denture base, Nanotubes.

## Introduction

Patients with edentulous arches are typically provided with complete dentures as a means to restore both appearance and functionality. A complete denture is made mainly from polymethyl methacrylate (PMMA) <sup>1</sup>. PMMA is a lightweight

material that is compatible, aesthetically pleasing, and easy to manufacture and fix. However, it is prone to microbial adhesion and fading, as well as being affected by exposure to different meals and beverages. It also has low wear resistance

and mechanical resistance, and a decrease in polymerization <sup>2</sup>.

In the last 10 years, denture fabrication has utilized new computer-assisted design and computer-assisted manufacturing (CAD-CAM) technology more frequently to circumvent the drawbacks of conventional techniques and materials <sup>3</sup>. The production of dental base resins by using three-dimensional (3D) printing technology has surged. Among its numerous benefits are precision and accuracy, which can result in improved tooth implantation and function. Furthermore, a short manufacturing cycle and low material waste translate into low manufacturing process costs <sup>4</sup>.

Two popular 3D-printing technologies used for denture production are stereolithography (SLA) and digital light processing (DLP). Nanofillers, such as metals, fibers, and oxides, enhance the mechanical and physical characteristics of resin-based materials, resulting in the production of nanocomposites with enhanced properties <sup>5</sup>. Recent efforts have primarily concentrated on augmenting the quantity of fillers to enhance the mechanical properties. The comprehensive performance of nanocomposites depends on various factors, including the intrinsic properties and type of polymers used, the processing technology of the composites, the dispersion and concentration of nanoparticles in the polymer matrix, the size of the nanoparticles, and the interfacial compatibility between the nanoparticles and the polymer matrix <sup>6</sup>.

Several adverse effects have been documented, such as reduced compatibility, the creation of voids that result in porosity, and the clustering of nanoparticles (NPs) that can cause areas of concentrated stress, ultimately leading to the initiation of crack propagation and fractures <sup>7</sup>. Carbon nanotubes (CNTs) can serve as fillers at low concentrations due to their ability to efficiently transmit loads in the interphase and enhance reinforcement. CNTs have attracted significant interest in the development of innovative materials owing to their distinctive characteristics, such as a large aspect ratio, extremely low weight, hardness, high tensile strength, outstanding electrical conductivity, and remarkable chemical and thermal stability <sup>8</sup>.

## Materials and methods

The low thermal conductivity of acrylic resin (about 0.2 W/m/°C) poses significant challenges during denture processing. In contrast to base materials for gold or cobalt alloys, the heat generated in acrylic resin does not effectively dissipate, leading to temperatures that may cause porosity during manufacturing <sup>9</sup>. For patients, low thermal conductivity may affect their sensory experience, as the palate covered by the denture base cannot sense the transitional changes in temperature effectively. This change in sensory perception may affect the patient's acceptance of acrylic dentures, especially during mastication, because it changes how the patient experiences the temperature of food <sup>10</sup>.

Various efforts have been undertaken to enhance the thermal characteristics of acrylic by incorporating fillers, such as tin, aluminum, and copper, or by introducing whiskers into the acrylic resin matrix <sup>9</sup>. While no perfect material has been found, acrylic resin is widely utilized as the primary dental base material. Acrylic resin's thermal conductivity, which is one of its drawbacks, has only been investigated in a limited number of studies. Further research is required <sup>11</sup>. Ensuring that the surface roughness of denture substrates remains within acceptable values is crucial to prevent the buildup of plaque, colonization by bacteria, and discoloration <sup>12</sup>. While it may be challenging to prevent surface permeability in digital manufacturing due to the characteristics of object production <sup>13</sup>, studies have demonstrated that surfaces with roughness values exceeding 0.2  $\mu\text{m}$  increase the rate at which bacteria colonize. The roughness observed is an inherent outcome of the layer-by-layer fabrication process employed in 3D printing technology <sup>14</sup>. Hardness is another important parameter used to evaluate when testing mechanical properties. Acrylic resin becomes harder and harder at scratching and abrasion.

To the best of the authors' knowledge, no prior research has examined the impact of incorporating CNTs into 3D-printed resins on thermal conductivity, surface roughness, and hardness. The null hypothesis of this study postulated that incorporating 0.5–0.7% by weight of CNTs would not result in a substantial impact on the physical and mechanical properties of 3D-printed denture base materials.

Based on earlier research <sup>15</sup>, the sample size was determined using G\*Power software (3.1.9.7; Heinrich-Heine-Universität Düsseldorf) with the following parameters:  $\alpha$ : 0.05, power: 0.90, effect size  $f$ : 0.7, and sample size for each group: 10. Ninety samples were printed using (Microlay Versus 385 dental printer, EU): 30 disc-shaped specimens for the thermal conductivity test with 40 mm diameter and 7 mm thickness according to the manufacturer's instructions, another 30 square-shaped specimens for the surface roughness test, and 30 squares for the hardness test with dimensions of 12 mm height, 12 mm width and 3 mm diameter according to ISO, 20795-1:2013. For each test the samples were divided into three groups ( $n=10$ ) according to CNTs percentage by weight (0%, 0.5%, 0.7%) <sup>16</sup>. For 0.7 percent of CNTs, the authors examined a percentage not previously investigated in other studies, to assess its effect on the physical and mechanical properties of 3D-printed denture base material.

CNTs with a purity of >99 wt. %, multiwalled carbon nanotubes (USA, Cambridgeport, VT 05141) with an average diameter of 37.4 nm were verified by a particle size analyzer and applied in certain weight-based concentrations to the 3D manufactured denture base material.

A stereolithography (STL) file was exported from the Microform computer program and transferred to

a digital light processing (DLP) open system microlay versus 385 3D-printer to print a pale pink denture foundation resin (Optiprint Laviva, Dentona Company, Germany). To reduce the viscosity of the resin, pure resin was placed on a mechanical mixer machine for 120 minutes before adding CNTs. The CNTs in the specified concentrations were added and distributed into several bottles, stirring continuously for 30 minutes at 60°C in a magnetic stirrer (Stuart scientific, UK). Finally, the mixture was stirred for 8 hours at room temperature to create a homogenous mixture for the printing process <sup>17</sup>. Following production guidelines, each layer was printed in (1.61) seconds per slice in the vertical Z axis at a layer thickness of 50  $\mu$ m. After the printing, the samples were then cleaned using 99.9% isopropyl alcohol, then dipped into glycerol, before being subjected to a UV light polymerization unit for 20 minutes to complete the process of polymerization <sup>18</sup>. After that, the support structures were removed using low-speed rotary instruments. Then, specimens were finished with silicon carbide grinding paper sequentially (800, 1500, and 2000 grit) and rinsed with water, finally polished with a lathe polishing tool (Fig. 1). To ensure that the same preparatory conditions were applied, a single operator completed the entire procedure. Before testing, the specimens were submerged in distilled water for 48 hours at 37°C <sup>19</sup>.

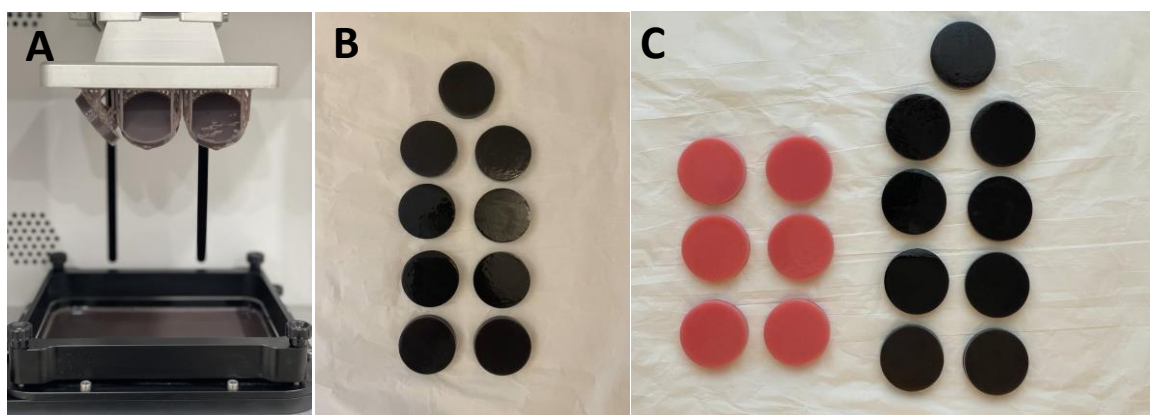


**Figure 1. The specimens after completing (A) The printing process (B) The finishing and polishing process (C) View of the color difference between the control and experimental groups.**

### Testing procedure

#### Thermal conductivity test

An extensively used standard method (ISO 22007-2;2022) for determining a material's thermal characteristics, particularly its thermal conductivity ( $k$ ), is the hot disc transient plane source (TPS)

method <sup>20</sup> (Thermal constants analyser TPS 500, Sweden). Using Hot's disc fixture instructions from the Technical University's Materials Engineering department, thirty samples were made. The disc samples were 7 mm thick and 40 mm in radius. While there are no special preparation requirements

for TPS specimens, the specimen has to be smooth and have a diameter of at least 3 cm to cover the probe sensor<sup>21</sup>. A thin metal foil disc (prepared with the same diameter of the sample and have thickness equal to 5mm) with a bifilar spiral pattern is used in the hot disc TPS technology as both the electrical resistive heater and the temperature sensor. The hot disc sensor is placed between two identical samples to be examined throughout the experiment, and a stepwise current is applied to the sensor to induce a stepwise Joule heating that produces a dynamic temperature<sup>20</sup>.

$$Cp = \frac{K}{D_{th}}$$

Where:  $D_{th}$  = Thermal diffusivity ( $\text{mm}^2 / \text{s}$ ).  $Cp$  = Specific heat at constant pressure ( $\text{MJ}/\text{m}^3 \text{K}$ ).

$K$  = Thermal conductivity ( $\text{W}/\text{m.K}$ ).

### Surface roughness test

Thirty samples were printed in compliance with ISO 20795-1:2013 specifications. The sample had a thickness of 3 mm and a dimension of 12 mm by 12 mm<sup>22</sup>. A contact profilometer (JIMTEC, JITAI8101, China) was used in this investigation to quantify surface roughness with a resolution of  $0.01 \mu\text{m}$ . The tool has a surface analyzer—a sensitive diamond tip—that allows it to track altitudes of the surface characteristics. Three readings per sample were taken, the device was adjusted so that the stylus touched the sample surface only three times<sup>23</sup>. The digital scale reading automatically appeared when the stylus was allowed to touch the sample's initial area while it was on a steady, stiff surface. The stylus touched the first point after moving around the designated surface (11 mm).

### Surface hardness test

Thirty samples were manufactured in compliance with ISO 20795-1:2013 requirements. The specimens' measurements matched those of the specimens with surface roughness<sup>22</sup>. A Shore D durometer (DIN ISO 7619, DIN EN ISO 868, DIN 53505, ASTM D 2240; Elcometer, Aalen, Germany) that has been approved for use with acrylic resins

was used to assess the surface hardness. The test load was 25 g applied on the samples for 10 seconds<sup>24</sup>. The major part of this instrument is a 0.8 mm diameter spring-loaded indenter. The indenter-equipped digital scale has a graduation range of zero to one hundred. The suggested technique called for applying a rapid, hard pressure to the indenter. The center and two ends of each specimen were measured independently, and the mean of these three measurements was utilized<sup>25</sup>.

### Field emission Scanning electron microscopy (FESEM)

The CNT dispersion pattern within the 3D printed resin material was examined using a FESEM (FEI, INSPECT F 50, Eindhoven, Netherlands) equipment. Three representatives' samples were analyzed, one for each group (0.5wt% and 0.7wt% for the control).

### Fourier transforms infrared spectroscopy (FTIR)

To ascertain whether there is any chemical interaction between the CNTs and the 3D printed resin material, FTIR (spectrometer—Spectrum Two, Perkin Elmer, USA) was used for the analysis. Three samples were analyzed, one for each group. (0.5wt% and 0.7wt% for the control). The range of the resolution was  $400\text{--}4000 \text{ cm}^{-1}$ .

### Statistical Analysis

The findings for the present research were analyzed using the GraphPad Prism software (version 9.0). The inferential analysis involved conducting a one-way ANOVA to compare the mean values of all groups. Additionally, the Shapiro-Wilk's test was used to assess the normal distribution of the data, while the Brown-Forsythe test was employed to evaluate the homogeneity of variance. The Bonferroni test was conducted to identify the specific significant differences among the groups. A  $P$  value greater than 0.05 ( $P > 0.05$ ) was deemed to be statistically insignificant (NS), while a  $P$  value of 0.05 or less was interpreted as statistically significant (S).

## Results

### Thermal conductivity test

Calculations were conducted using descriptive statistics, such as the mean and standard deviation. When CNTs were added, the experimental groups' mean values rose in comparison with the control

group. The group with 0.7% weighted CNTs had the highest mean, 0.4395 ( $\text{W}/\text{m.K}$ ), whereas the control group's mean was 0.3745 ( $\text{W}/\text{m.K}$ ). Significant findings were obtained via a one-way ANOVA table comparing the means of all investigated groups



(Table 1). The multiple comparison (Bonferroni test) revealed significant differences between the control and 0.5% by weight of CNTs, with a significant value for 0.7% by weight of CNTs as compared with the control (Table 2 and Fig. 2).

**Table 1. The mean values, standard deviation and ANOVA of thermal conductivity test**

Study groups	Control	0.5%	0.7%
Mean	0.3745	0.4278	0.4395
Std. deviation	0.0268	0.0288	0.0383
Minimum	0.3380	0.4090	0.3820
Maximum	0.4260	0.5020	0.4890
One-way F	11.96		
Anova P value	<0.0002		

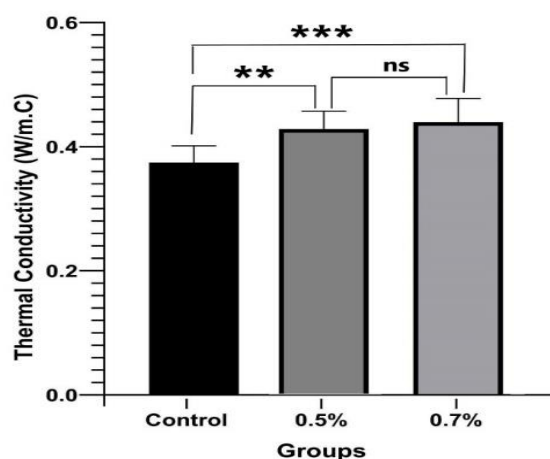


**Figure 2. Bar chart for thermal conductivity test.** \*\*\* high significant P value = 0.0003, \*\* significant P value = 0.0025, ns = not significant P value = 0.9999

**Table 2. Bonferroni's multiple comparison of thermal conductivity test**

Bonferroni's multiple comparisons test	Mean Diff.	Adjusted P Value
Control vs. 0.5%	-0.05330	0.0025
Control vs. 0.7%	-0.06500	0.0003
0.5% vs. 0.7%	-0.01170	>0.9999

### Surface roughness test

The mean and standard deviation were among the descriptive statistics that were employed. When CNTs were added, the experimental group's mean values increased in comparison to the control group, according to the results. The group with 0.7% weighted CNTs had the greatest mean, 0.3950, whereas the control group had the lowest mean, 0.2658 (Table 3). Significant findings were found

when the means of the experimental groups' data were compared using an ANOVA table. The multiple comparisons (Bonferroni test) revealed significant differences between the control and 0.5% by weight of CNTs, with a significant value for 0.7% by weight of CNTs as compared to the control groups (Table 4 and Fig. 3).

**Table 3. The mean values, standard deviation, and ANOVA of surface roughness test.**

Study groups	Control	0.5%	0.7%
Mean	0.2658	0.3382	0.3950
Std. deviation	0.0586	0.0364	0.0525
Minimum	0.2150	0.2580	0.3180
Maximum	0.3830	0.3840	0.4990
One-way F	16.73		
Anova P value	<0.0001		

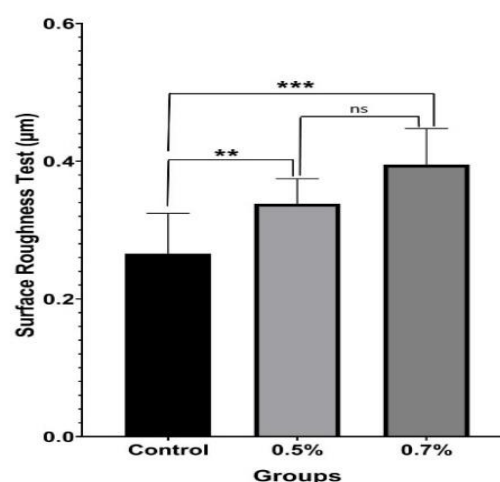


**Figure 3. Bar chart for Surface roughness test.** \*\*\*high significant P value <0.0001, \*\*significant P value = 0.0096, ns = not significant P value = 0.0518

**Table 4. Bonferroni's multiple comparison of surface roughness test.**

Bonferroni's multiple comparisons test	Mean Diff.	Adjusted P Value
Control vs. 0.5%	-0.07240	0.0096
Control vs. 0.7%	-0.1292	<0.0001
0.5% vs. 0.7%	-0.05680	0.0518

### Surface hardness test

The mean and standard deviation were among the descriptive statistics that were employed. When CNTs were added, the experimental group's mean values increased in comparison to the control group, according to the results. The group with 0.7% by

weight CNT content had the highest mean, 88.24, whereas the control group's mean was 85.76. Significant findings were found when the means of the experimental groups' data were compared using an ANOVA table (Table 5). Using the Bonferroni multiple comparisons test, significant differences were found between the control and 0.5% by weight of CNTs. Moreover, significant values were found for 0.7% by weight of CNTs when compared to the control group (Table 6 and Fig. 4).

**Table 5. Mean values, standard deviation, and ANOVA of surface hardness test.**

Study groups	Control	0.5%	0.7%
Mean	85.76	87.12	88.24
Std. deviation	0.9969	0.8954	0.3627
Minimum	84.20	85.00	87.60
Maximum	87.20	88.20	88.80
One-way F	24.01		
P value	<0.0001		

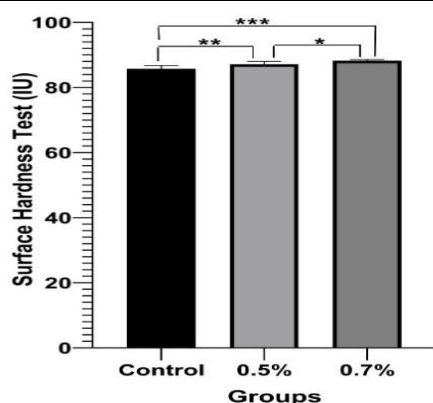


**Figure 4. Bar chart for surface hardness test. \*\*\* high significant P value <0.0001, \*\* significant P value = 0.0023, \* significant P value = 0.0127**

**Table 6. Bonferroni's multiple comparison of surface hardness test**

Bonferroni's multiple comparisons test	Mean Diff.	Adjusted P Value
Control vs. 0.5%	-1.360	0.0023
Control vs. 0.7%	-2.480	<0.0001
0.5% vs. 0.7%	-1.120	0.0127

### FTIR result

As shown in Fig. 5, the addition of CNTs didn't affect the spectrum range of the resin that was 3D printed (no chemical interaction). One test sample evaluation was sufficient to compare the results with

the control group; the FTIR was only utilized to confirm whether or not there was a chemical reaction. The FTIR spectrum shows the absorption peaks corresponding to the vibrational modes of the functional groups in the sample. The characteristic peaks of the common functional groups, such as OH, C=O, NH, CH, etc., can be identified to confirm the presence of specific chemical bonds. As shown in Fig. 5, 0.5 wt.% and 0.7 wt.% of CNTs with 3D printed acrylic resin, a peak was present around 3410  $\text{cm}^{-1}$  due to the N-H bending vibration in  $\text{NH}_3$ . Because the network structure's creation produced a steric effect, the weak peak at 2927  $\text{cm}^{-1}$  which was attributed to the O-H bonds. A sharp peak was evident around 1100  $\text{cm}^{-1}$  due to C=O vibrations. A strong peak around 1728  $\text{cm}^{-1}$  is due to C=O stretching vibrations. Peaks around 1635- 1532  $\text{cm}^{-1}$  are due to the C=C stretching vibrations in the aromatic ring. Weak peaks are present at 1457  $\text{cm}^{-1}$ , 797  $\text{cm}^{-1}$ , 619  $\text{cm}^{-1}$  and 486  $\text{cm}^{-1}$  N – H, C-O-H, C – Cl, C – Br and C – I respectively.

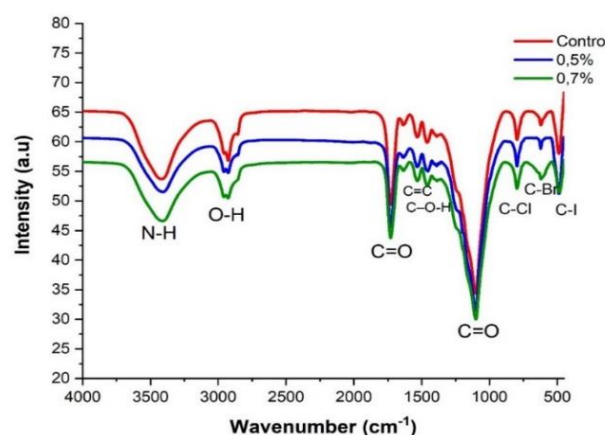


**Figure 5. Denture resin 3D printed with (0%, 0.5%, and 0.7%) by weight CNTs addition. FTIR spectra. The X and Y axes stand for wavenumber  $\text{cm}^{-1}$  and transmittance percentage, respectively. The bonds shown in the graphic match the wavenumber of its peak.**

### FESEM result

As seen in Fig. 6 (A), FESEM images amply proved that the nanotubes' diameter fell within the nanometer range. Fig. 6 (B) represents the resin as it was originally structured (the control) before any changes were made. Additionally, as seen in Fig. 6 (C and D), FESEM proved the 0.5% and 0.7% CNTs nanotubes' effective integration into the 3D printed resin substrate. The control 3D printed resin in Fig. 6 (B) of the sample surfaces at 250 $\times$  magnification

appeared to have wide, dispersed pores with irregularities, whereas in Fig. 6 (C and D) of the 3D resin with 0.5% and 0.7%, respectively, the CNTs demonstrated more compact and regular surface with more diminished pores and roughness. These

differences appeared most probably due to CNTs dispersions within the 3D printed denture base materials, which are homogenous at low concentrations (Fig. C) and cluster formation at higher concentrations (Fig. D).

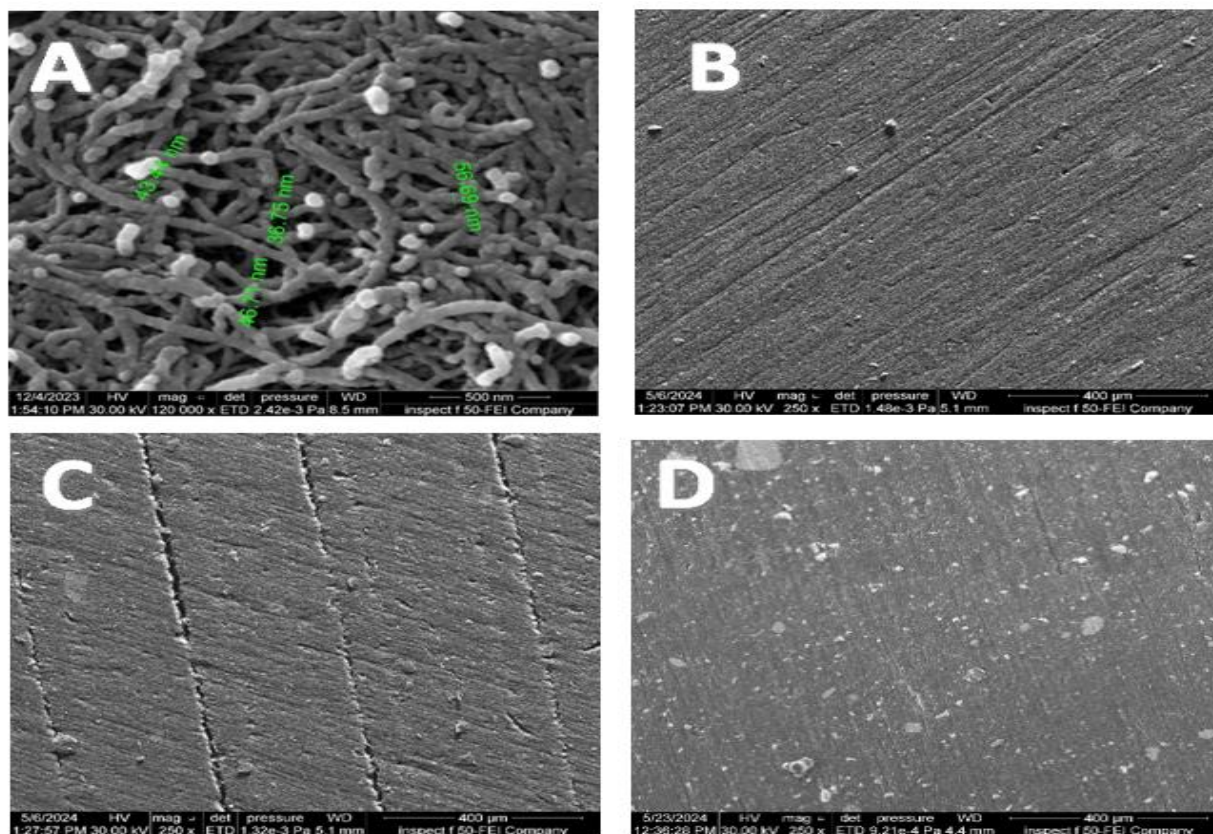


**Figure 6. FESEM micrograph (A) CNTs powder at 120 000x magnification (500 nm); (B) control 3D-printed resin specimen at 250x magnification (400 μm); (C) 3D printed resin specimen reinforced with 0.5% CNTs at 250x magnification; (D) specimen reinforced with 0.7% CNTs at 250x magnification.**

## Discussion

Thermal conductivity is a key property of dental materials that determines how quickly heat can be transferred across a material's cross-section at a specific moment in time <sup>26</sup>. The thermal conductivity is influenced by various factors, including the inherent heat conductivity of fillers and matrices, in addition to the composition, dimensions, forms, and loading amounts of fillers <sup>27</sup>. The groups with weight percentages of 0.5% and 0.7% show the highest enhancements in thermal conductivity compared to the control group. Increased concentration leads to the formation of compact nanoparticle structures within matrices that are rigid, substantial, and facilitate the conduction of heat. Conversely, the interaction between

nanoparticles increases as the amount of filler material increases <sup>28</sup>.

The phenomenon observed is a consequence of the thermal conduction properties inherent in the structural composition of carbon nanotubes. The thermal conductivity of a solid is directly influenced by the mobility of electrons, phonons, and photons, which is widely recognized. Phonons are considered to be the main carriers of thermal energy in the case of CNTs, while the contribution of electrons is almost negligible <sup>29</sup>. A phonon refers to a fundamental vibrational movement that is characterized by quantum mechanics. It involves a regular oscillation of a lattice composed of atoms or



molecules, typically observed in solids and certain liquids, occurring at a specific frequency.

In contrast, polymers exhibit significantly lower thermal conductivity compared to CNTs<sup>13</sup>. The typical range of values is between 0.175 and 0.30 W/m K. Phonons are the main agents responsible for transferring thermal energy in polymers, and they exhibit a significantly low thermal conductivity. The reason for this is that CNTs have a relatively short mean free path for phonons, typically only a few angstroms, due to their dispersion caused by numerous defects<sup>30</sup>.

Despite the significant difference in thermal conductivities between polymers and CNTs, the addition of CNTs to polymer matrices only slightly increases their thermal conductivity<sup>31</sup>. The occurrence of interfacial thermal resistance at the interface between the polymer matrix and CNTs has been attributed to this phenomenon. The observed heat flow barrier may be attributed to variations in the phonon spectra of the two phases and potential weak contact at the interface, which are dependent on the atomic structure and density<sup>32</sup>.

The scattering of phonons at the interface between the two materials occurred as a result of the differences in their phonon vibration spectra. The probability of phonon transmission after scattering depends on the degree of overlap between the available phonon energy levels in the different phases and is connected to the thermal resistance at the interface. Research on heat transfer at the interface between CNTs and liquid octane has revealed that energy exchange primarily occurs between liquid polymers and CNT phonon modes that have similar vibration frequencies. This finding provides strong support for the proposed hypothesis<sup>33</sup>. Previous research has also shown similar results for the interaction between CNTs and water<sup>34</sup>.

Multiwalled carbon nanotube (MWCNT)-epoxy was produced by Singh et al. using a mixing process<sup>35</sup>. Compared to pure epoxy, the thermal conductivity of epoxy with 0.5 weight percent MWCNTs is 72.5% greater. When MWCNTs and graphene nanoplatelets hybrid fillers are introduced to epoxy, as Chang et al. did<sup>36</sup>, the epoxy's thermal conductivity increases by 287% at 1.525 weight percent MWCNTs and 4.575 weight percent GNPs. The type of filler, the dispersion of the filler, and the thermal conductivity

channel between the fillers are some of the elements that affect a composite's thermal conductivity.

An increase in the filler content of MWCNTs-COOH in styrene acrylic resin leads to a greater aggregation of CNTs, resulting in a decrease in thermal conductivity. When the concentration of the filler is increased to 2.5wt%, the thermal conductivity decreases to 0.2004 W/(m·K)<sup>37</sup>. The addition of CNTs to the composite creates interphase layers that effectively decrease the potential for phonon scattering at the interface between carbon fibers and the polymer matrix<sup>38</sup>.

When the hardness of a material is low, it is more prone to scratches, damage to the resin surface, and changes in dimensions that can occur from brushing dentures or chewing hard foods. The hardness of the specimen's surface is an indicator of how well it can withstand abrasion and reflects the strength of the material's surface. The mean hardness and mean surface roughness of the 3D-printed denture bases range from 30.17 to 34.62 Vickers hardness number (VHN) and 0.12 to 0.22  $\mu\text{m}$ , respectively<sup>39</sup>. In comparison to the control group (85.76), the test groups' Shore D hardness values increased as CNT concentrations increased, particularly at the higher 0.7% concentration (88.24). Furthermore, the outcome shows that the shore D values of the 3D printed denture base resin are not significantly affected by the inclusion of CNTs. The presence of solid particles inside the matrix has caused the material to become more rigid, which accounts for the rise in hardness. The random dispersion of solid particles in the acrylic matrix may also be contributing to the increase<sup>40</sup>. Additionally, the increase in hardness is attributed to the overlap and stacking of polymer molecules, which restrict their movement. This restriction enhances the material's resistance to scratches, cuts, and plastic deformation. Hardness in materials is largely influenced by the type of forces binding the atoms together. In this case, the strong linkages at the interface between CNTs and the 3D-printed resin improve the coherence of the mixture, leading to an increase in hardness<sup>41</sup>.

These findings supported the research put out by Hall and Petch, which found that a finer and smaller grain boundary led to a considerable rise in the hardness values<sup>42</sup>. The CNTs' grain boundaries in the composites were fine because of the lower particle



sizes. When further chemicals are added, the microstructure of the composite gets finer. As a result, the samples get harder as the filler dosage increases.

According to Balos et al., the accumulation of nanoparticles on the specimen surface, particularly at a higher concentration, maybe the reason for the increase in its hardness. The dense polymethylmethacrylate layer surrounding these accumulations immobilizes the PMMA layer, making it resilient to indentation <sup>43</sup>.

The findings contradict the findings of Gad et al., who claimed that adding aluminum, silanized nanoTiO<sub>2</sub>, or nanoSiO<sub>2</sub> would enhance the surface hardness of PMMA. On the other hand, they found that adding carbon nanotubes reduced surface hardness <sup>44</sup>.

*Candida albicans* adheres to and is retained on surfaces roughened by scratches, which is particularly significant in the pathophysiology of denture-induced stomatitis. Plaque buildup should thus be prevented or avoided by a substance with a smooth polished surface. The modified 3D printed resin's surface roughness rose somewhat when compared to the control group. This might be related to the relatively high filler loading quantity, which could result in the production of certain filler aggregates on the surface, as well as the difference in particle sizes between the nano fillers and the base material for acrylic dentures <sup>45</sup>. When compared to the control group (0.2658), the roughness increased as the concentration of CNTs rose, particularly at the higher 0.7% concentration (0.3950).

Surface roughness tests revealed that the Ra value significantly increased for rough (220 grit) specimens compared to smooth (2400 grit) specimens. This increase in roughness was found to be associated with the incorporation of carbon nanotubes CNT <sup>46</sup>.

The present findings agree with Kim et al, in which the surface roughness and water contact angle increased with increasing CNTs incorporation <sup>46</sup>. In another conducted study, adding 1.5% single walled

CNTs into heat cured acrylic resin caused non-significant effect on the surface roughness when compared with the control group <sup>47</sup>.

Our findings contradict the findings of Mhaibes et al., who claimed that the addition of 1.0 and 1.5 wt.% TiO<sub>2</sub> nanotubes to 3D-printed denture base materials caused a considerable reduction in the surface roughness of the nanocomposites compared to that of the control group <sup>48</sup>.

FTIR measurements were carried out both before and after the CNTs were added. There was no chemical reaction since the spectral range did not change before or after the addition. In this instance, fillers and resin combine to produce the single interaction, which is defined as a physical reaction (hydrogen bond or Van der Waals bond) <sup>49</sup>. The vibration of the existent connections somewhat changed as a result of this interaction.

As the filler percentage increased, the FESEM showed well-dispersed CNTs inside the resin matrix with some agglomeration. These findings were consistent with Al-Sammraie and Fatalla study's findings <sup>50</sup>.

This study's limitations included the use of only two CNTs concentrations and a single type of 3D-printed denture base resin. A higher concentration of CNTs would provide a better understanding of the behavior of CNTs within the 3D-printed resin for denture base material. Thus, it is necessary to conduct in vivo testing to verify the information clinically.

It is recommended to investigate the effects of CNTs on other characteristics of 3D-printed denture base materials, including color stability, water sorption, solubility, wettability, shear bonding, flexural strength, and impact strength, alongside assessments of bacteria and *Candida albicans* adherence and the biocompatibility testing. Equally important is the investigation of how different processing parameters, such as optimal printing orientation, curing and post-curing durations, layer thickness, polishing methods, and specimen storage, affect the properties of 3D-printed resin.

## Conclusion

Adding carbon nanotubes (CNTs) to 3D-printed denture base resin significantly enhances its hardness

and thermal conductivity; the degree of improvement is directly linked to the CNT concentration.

However, the surface roughness increased as more filler are added. In contrast, further research is necessary to fully understand how surface roughness

affects the mechanical characteristics of the base material used in 3D-printed dentures and how CNTs may influence it.

### Author's Declaration

- Conflicts of Interest: None.
- We hereby confirm that all the Figures and Tables in the manuscript are ours. Furthermore, any Figures and images, that are not ours, have been included with the necessary permission for re-publication, which is attached to the manuscript.

- No animal studies are present in the manuscript.
- No human studies are present in the manuscript.
- Ethical Clearance: The project was approved by the local ethical committee at University of Baghdad.

### Author's Contributions statement

All authors contributed to the design and implementation of the research, to the analysis of the results and to the writing of this manuscript: R.R.K. and A.A.F. conceived of the presented idea. R.R.K. Data collection and analysis. A.A.F., M.A.R. and

Y.J. verified the analytical methods. R.R.K: wrote the manuscript with contributions from all authors. Y.H.B., M.A.R and J.Y.A. provided critical revisions. A.A.F., Y.J. and J.Y.A. provided project management and oversight.

### References

1. Zeidan AA, Sherif AF, Baraka Y, Abualsaud R, Abdelrahim RA, Gad MM et al. Evaluation of the Effect of Different Construction Techniques of CAD-CAM Milled, 3D-Printed, and Polyamide Denture Base Resins on Flexural Strength: An In Vitro Comparative Study. *J Prosthodont.* 2003; 32(1): 77–82. <https://doi.org/10.1111/jopr.13514>
2. Gökay GD, Durkan R, Oyar P. Evaluation of physical properties of polyamide and methacrylate based denture base resins polymerized by different techniques. *Niger. J Clin Pract.* 2021; 24(12): 1835–1840. [https://doi.org/10.4103/njcp.njcp\\_469\\_20](https://doi.org/10.4103/njcp.njcp_469_20)
3. Alghazzawi TF. Advancements in CAD/CAM technology: Options for practical implementation. *J Prosthodont Res.* 2016; 60(2): 72–84. <https://doi.org/10.1016/j.jpor.2016.01.003>
4. Tian Y, Chen C, Xu X, Wang J, Hou X, Li K et al. A review of 3D printing in dentistry: Technologies, affecting factors, and applications. *Scanning.* 2021; 9950131. <https://doi.org/10.1155/2021/9950131>
5. Unkovskiy A, Schmidt F, Beuer F, Li P, Spintzyk S, Kraemer Fernandez P. Stereolithography vs. direct light processing for rapid manufacturing of complete denture bases: An in vitro accuracy analysis. *J Clin Med.* 2021; 10(5): 1070–1082. <https://doi.org/10.3390/jcm10051070>
6. Al-Rawi KR, Taha SK. The Effect of nano particles of TiO<sub>2</sub>-Al<sub>2</sub>O<sub>3</sub> on the mechanical properties of epoxy Hybrid nanocomposites. *Baghdad Sci J.* 2015; 12(3): 597–602. <https://doi.org/10.21123/bsj.2015.12.3.597-602>
7. Al-Sammraie MF, Fatalla AA, Atarchi ZR. Assessment of the correlation between the tensile and diametrical compression strengths of 3D-printed denture base resin reinforced with ZrO<sub>2</sub> nanoparticles. *J Baghdad Coll Dent.* 2024; 36(1): 44–53. <https://doi.org/10.26477/jbcd.v36i1.3590>
8. Hoyos-Palacio LM, Castro DP, Ortiz-Trujillo IC, Palacio LE, Upegui BJ, Mora NJ et al. Compounds of carbon nanotubes decorated with silver nanoparticles via in-situ by chemical vapor deposition (CVD). *J Mater Res Technol.* 2019; 8(6): 5893–5898. <https://doi.org/10.1016/j.jmrt.2019.09.062>
9. Abdulhamed AN, Mohammed AM. Evaluation of thermal conductivity of alumina reinforced heat cure acrylic resin and some other properties. *J Bagh Coll Dent.* 2010; 22(3): 1–6.
10. Messersmith PB, Obrez A, Lindberg S. New acrylic resin composite with improved thermal diffusivity. *J Prosthet Dent.* 1998; 79(3): 278–284. [https://doi.org/10.1016/S0022-3913\(98\)70238-0](https://doi.org/10.1016/S0022-3913(98)70238-0)
11. Kul E, Aladağ LI, Yesildal R. Evaluation of thermal conductivity and flexural strength properties of poly (methyl methacrylate) denture base material reinforced with different fillers. *J Prosthet Dent.* 2016; 116(5): 803–810. <https://doi.org/10.1016/j.prosdent.2016.03.006>
12. Quezada MM, Salgado H, Correia A, Fernandes C, Fonseca P. Investigation of the effect of the same polishing protocol on the surface roughness of denture base acrylic resins. *Biomedicines.* 2022; 10(8): 1971–1980. <https://doi.org/10.3390/biomedicines10081971>
13. Alharbi N, Osman R. Does Build Angle Have an Influence on the Surface Roughness of Anterior 3D-

- Printed Restorations? An In Vitro Study. *Int J Prosthodont.* 2021; 34(4): 505–510. <https://doi.org/10.11607/ijp.7100>
14. Al-Dwairi ZN, Al Haj Ebrahim AA, Baba NZ. A comparison of the surface and mechanical properties of 3D printable denture-base resin material and conventional polymethylmethacrylate (PMMA). *J Prosthodont.* 2023; 32(1): 40–48. <https://doi.org/10.1111/jopr.13491>
15. Abdullah HA, Abdul-Ameer FM. Evaluation of some mechanical properties of a new silicone elastomer for maxillofacial prostheses after addition of intrinsic pigments. *Saudi Dent J.* 2018; 30(4): 330–336. <https://doi.org/10.1016/j.sdentj.2018.05.006>
16. Ameer AK, Mousa MO, and Ali WY. Hardness and wear of polymethyl methacrylate filled with multi-walled carbon nanotubes as denture base materials. *J Egypt Soc Tribol.* 2017; 14(3): 66–83.
17. Gad MM, Al-Harb FAi, Akhtar S, Fouda SM. 3D-printable denture base resin containing SiO<sub>2</sub> nanoparticles: An in vitro analysis of mechanical and surface properties. *J Prosthodont.* 2022; 31(9): 784–790. <https://doi.org/10.1111/jopr.13483>
18. Lin CH, Lin YM, Lai YL, Lee SY Mechanical properties, accuracy, and cytotoxicity of UV-polymerized 3D printing resins composed of Bis-EMA, UDMA, and TEGDMA. *J Prosthet Dent.* 2020; 123(2): 349–354. <https://doi.org/10.1016/j.prosdent.2019.05.002>
19. Al-Sammraie MF, Fatalla AA. The Effect of ZrO<sub>2</sub> Nanoparticles Addition on Candida Adherence and Tensile Strength of 3D Printed Denture Base Resin. *J Nanostructures.* 2023; (13)2: 544–552. <https://doi.org/10.22052/JNS.2023.02.024>
20. Zheng Q, Kaur S, Dames C, Prasher RS. Analysis and improvement of the hot disk transient plane source method for low thermal conductivity materials. *Int J Heat Mass Transf.* 2020; 151: 119331. <https://doi.org/10.1016/j.ijheatmasstransfer.2020.11.9331>
21. Kareem YM, Hamad TI, Matheel AR. Evaluating the effect of barium titanate nanofiller addition on the thermal conductivity and physio-mechanical properties of maxillofacial silicone. *J Baghdad Coll Dent.* 2024; 36(2): 20–33. <https://doi.org/10.26477/jbcd.v36i2.3674>
22. Al-Douri ME Sadoon MM. Flexural Strength, Hardness and Surface Roughness of 3D Printed Denture Base Resin Reinforced by Zinc Oxide Nanoparticles. *J Res Med Dent Sci.* 2023; 11(01): 194–200.
23. Noori ZS, Al-Khafaji AM, Dabaghi F. Effect of tea tree oil on candida adherence and surface roughness of heat cure acrylic resin. *J Baghdad Coll Dent.* 2023; 35(4): 46–54. <https://doi.org/10.26477/jbcd.v35i4.3513>
24. Altaie SF. Tribological, microhardness and color stability properties of a heat-cured acrylic resin denture base after reinforcement with different types of nanofiller particles. *Dent Med Probl.* 2023; 60(2): 295–302. <https://doi.org/10.17219/dmp/137611>
25. AlFuraiji NH, Altaie SF, Qasim SS. Evaluating the influence of Ti6Al4V alloy particles on mechanical properties of heat-cured PMMA. *J Baghdad Coll Dent.* 2024; 36(2): 44–53. <https://doi.org/10.26477/jbcd.v36i2.3676>
26. Sakaguchi RL, Powers JM. *Craig's Restorative Dental Materials-E-Book: Craig's Restorative Dental Materials-E-Book.* Elsevier Health Sciences; 2011. 51–96.
27. Puskas JE, Foreman-Orlowski EA, Lim GT, Porosky SE, Evancho-Chapman MM, Schmidt SP et al. A nanostructured carbon-reinforced polyisobutylene-based thermoplastic elastomer. *Biomaterials.* 2010; 31(9): 2477–2488. <https://doi.org/10.1016/j.biomaterials.2009.12.003>
28. Devpura A, Phelan PE, Prasher RS. Percolation theory applied to the analysis of thermal interface materials in flip-chip technology. in *ITHERM 2000. The Seventh Intersociety Conference on Thermal and Thermomechanical Phenomena in Electronic Systems* (Cat. No. 00CH37069), IEEE, 2000;1: 21–28. <https://doi.org/10.1109/ITHERM.2000.866803>
29. Benedict LX, Louie SG, Cohen LM. Heat capacity of carbon nanotubes. *Solid State Commun.* 1996; 100(3): 177–180. [https://doi.org/10.1016/0038-1098\(96\)00386-9](https://doi.org/10.1016/0038-1098(96)00386-9)
30. Agari Y, Ueda A, Omura Y, Nagai S. Thermal diffusivity and conductivity of PMMA/PC blends. *Polymer.* 1997; 38(4): 801–807. [https://doi.org/10.1016/S0032-3861\(96\)00577-0](https://doi.org/10.1016/S0032-3861(96)00577-0)
31. Guthy C, Du F, Brand S, Winey KI, Fischer JE. Thermal conductivity of single-walled carbon nanotube/PMMA nanocomposites. *J Heat Transfer.* 2007; 129(8): 1096–1099. <https://doi.org/10.1115/1.2737484>
32. Han Z, Fina A, “Thermal conductivity of carbon nanotubes and their polymer nanocomposites: A review. *Prog Polym Sci.* 2011; 36(7): 914–944. <https://doi.org/10.1016/j.progpolymsci.2010.11.004>
33. Shenogin S, Bodapati A, Xue L, Ozisik R, Keblinski P. Effect of chemical functionalization on thermal transport of carbon nanotube composites. *Appl Phys Lett.* 2004; 85(12): 2229–2231. <https://doi.org/10.1063/1.1794370>
34. Thomas JA, Iutzi RM, McGaughey AJH. Thermal conductivity and phonon transport in empty and water-filled carbon nanotubes. *Phys Rev B.* 2010; 81(4): 45413. <https://doi.org/10.1103/PhysRevB.81.045413>

35. Singh AK, Panda BP, Mohanty S, Nayak SK, Gupta MK. Study on metal decorated oxidized multiwalled carbon nanotube (MWCNT)-epoxy adhesive for thermal conductivity applications. *J Mater Sci Mater Electron*. 2017; 28: 8908–8920. <https://doi.org/10.1007/s10854-017-6621-3>
36. Chang HP, Liu HC, Tan CS. Using supercritical CO<sub>2</sub>-assisted mixing to prepare graphene/carbon nanotube/epoxy nanocomposites. *Polymer*. 2015; 75: 125–133. <https://doi.org/10.1016/j.polymer.2015.08.023>
37. Jia F, Fagbohun EO, Wang Q, Zhu D, Zhang J, Gong B et al. Improved thermal conductivity of styrene acrylic resin with carbon nanotubes, graphene and boron nitride hybrid fillers. *Carbon Resour Convers*. 2021; 4: 190–196. <https://doi.org/10.1016/j.crcon.2021.05.001>
38. Mazov I, Burmistrov I, Il'inykh I, Stepashkin A, Kuznetsov D, Issi J. Anisotropic thermal conductivity of polypropylene composites filled with carbon fibers and multiwall carbon nanotubes. *Polym Compos*. 2015; 36(11): 1951–1957. <https://doi.org/10.1002/pc.23104>
39. Gad MM, Fouda SM, Abualsaud R, Alshahrani FA, Al-Thobity AM, Khan SQ et al. Strength and surface properties of a 3D-printed denture base polymer. *J Prosthodont*. 2022; 31(5): 412–418. <https://doi.org/10.1111/jopr.13413>
40. Alnamel HA, Mudhaffer M. The effect of Silicon di oxide Nano-Fillers reinforcement on some properties of heat cure polymethyl methacrylate denture base material. *J Baghdad Coll Dent*. 2014; 26(1): 32–36.
41. Husaen SI. Mechanical properties of carbon nanotube reinforced Epoxy Resin composites. *Baghdad Sci J*. 2012; 9(2): 330–334. <https://doi.org/10.21123/bsj.2012.9.2.330-334>
42. Hansen N. Hall–Petch relation and boundary strengthening. *Scr Mater*. 2004; 51(8): 801–806. <https://doi.org/10.1016/j.scriptamat.2004.06.002>
43. Balos S, Pilic B, Markovic D, Pavlicevic J, Luzanin O. Poly (methyl-methacrylate) nanocomposites with low silica addition. *J Prosthet Dent*. 2014; 111(4): 327–334. <https://doi.org/10.1016/j.prosdent.2013.06.021>
44. Gad MM, Fouda SM, Al-Harbi FA, Näpänkangas R, Raustia A. PMMA denture base material enhancement: a review of fiber, filler, and nanofiller addition. *Int J Nanomedicine*. 2017; 3801–3812. <https://doi.org/10.2147/IJN.S130722>
45. Fatalla AA, Tukmachi MS, Jani GH. Assessment of some mechanical properties of PMMA/silica/zirconia nanocomposite as a denture base material. in *Institute of Physics. IOP Conf Ser . Mater Sci Eng*. 2020;987 12031. <https://doi.org/10.1088/1757-899X/987/1/012031>
46. Kim KI, Kim DA, Patel KD, Shin US, Kim HW, Lee JH et al. Carbon nanotube incorporation in PMMA to prevent microbial adhesion. *Sci Rep*. 2019; 9(1): 4921. <https://doi.org/10.1038/s41598-019-41381-0>
47. Ibrahim RA. The effect of adding single walled carbon nanotube with different concentrations on mechanical properties of heat-cure acrylic denture base material. *J Bagh Coll Dent*. 2015; 27(3): 28–32. <https://jbcd.uobaghdad.edu.iq/index.php/jbcd/article/view/802>
48. Mhaibes AH, Safi IN, Haider J. The influence of the addition of titanium oxide nanotubes on the properties of 3D printed denture base materials. *J Esthet Restor Dent*. 2024; 1-17. <https://doi.org/10.1111/jerd.13299>
49. Kareem YM, Hamad TI. Assessment of the antibacterial effect of Barium Titanate nanoparticles against *Staphylococcus epidermidis* adhesion after addition to maxillofacial silicone. *F1000Research*. 2023; 12: 385. <https://doi.org/10.12688/f1000research.132727.1>
50. Al-Sammraie MF, Fatalla AA. The effect of ZrO<sub>2</sub> NPs addition on denture adaptation and diametral compressive strength of 3D printed denture base resin. *Nanomed Res J*. 2023; 8(4): 345–355. <https://doi.org/10.22034/NMRJ.2023.04.003>



## تحليل التوصيل الحراري وخشونة السطح وصلابة راتينج الأكريليك المطبوع ثلاثي الأبعاد المقوى بأنابيب الكربون النانوية

رنين رعد خالد<sup>1</sup>، عبد الباسط أحمد فتح الله<sup>1</sup>، مثيل الرواس<sup>2</sup>، ينّي جوهاري<sup>2</sup>، يوو هين به<sup>3</sup>، جوهاري يب عبد الله<sup>4,5</sup>

<sup>1</sup> قسم التعويضات السنية، كلية طب الأسنان، جامعة بغداد، بغداد، العراق.

<sup>2</sup> وحدة التعويضات السنية، كلية علوم طب الأسنان، جامعة سينز الماليزية، كوبانج كيريان، ماليزيا.

<sup>3</sup> قسم طب الأسنان الترميمي، كلية طب الأسنان، جامعة كييانجسان ماليزيا، كوالالمبور، ماليزيا.

<sup>4</sup> مختبر التصوير القحفي الوجهي، كلية علوم الأسنان، الحرم الصحي، جامعة العلوم الماليزية، كوبانج كيريان، كوتا بهارو 16150، ماليزيا

<sup>5</sup> وحدة أبحاث الأسنان، مركز الأبحاث متعددة التخصصات، كلية طب الأسنان سافيتا، معهد سافيتا للعلوم الطبية والتقنية، جامعة سافيتا، تشيناي 602105، الهند.

### الخلاصة

إن مجال طب الأسنان في تطور مستمر، خاصة مع تكنولوجيا الطباعة ثلاثية الأبعاد. تهدف هذه الدراسة إلى تحليل كيفية تأثير قواعد أطقم الأسنان المصنوعة من مادة الراتنج ثلاثية الأبعاد على التوصيل الحراري، وخشونة السطح، وصلابة السطح عند إضافة أنابيب الكربون النانوية (CNTs) بنسب وزنية مختلفة. تمت إضافة الأنابيب النانوية الكربونية إلى راتنج أكريليك قاعدة طقم الأسنان المطبوع ثلاثي الأبعاد. تم تقسيم العينات إلى ثلاث مجموعات؛ 0.5% و 0.7% من الأنابيب النانوية الكربونية بالوزن ومجموعة مراقبة أخرى لا تحتوي على الأنابيب النانوية الكربونية المضافة. خضعت جميع العينات لاختبارات التوصيل الحراري وخشونة السطح وصلابة السطح. تم إجراء تحويلات فوربيه للتحليل الطيفي للأشعة تحت الحمراء وتحليلات المجهر الإلكتروني لمسح الانبعثات الميدانية، وتم تحليل البيانات عن طريق تحليل التباين (ANOVA) أحادي الاتجاه واختبارات المقارنة المتعددة. أدت إضافة الأنابيب النانوية الكربونية إلى راتنج قاعدة طقم الأسنان المطبوع ثلاثي الأبعاد إلى تحسين صلابة السطح والتوصيل الحراري مقارنة بمجموعة التحكم ويرتبط ذلك بتركيز الأنابيب النانوية الكربونية المضافة. ومع ذلك، زادت خشونة السطح مع زيادة الأنابيب النانوية الكربونية المضافة إلى الراتنج. تعمل إضافة الأنابيب النانوية الكربونية إلى راتنج قاعدة طقم الأسنان المطبوع ثلاثي الأبعاد على تحسين السلوك الميكانيكي للمادة، وخاصة التوصيل الحراري وصلابة السطح، ولكن ليس خشونة السطح. لذلك يجب توخي الحذر عند اختيار التركيز المناسب من الأنابيب النانوية الكربونية المراد إضافتها إلى راتنج الطباعة ثلاثية الأبعاد في تحسين خصائص المواد

**الكلمات المفتاحية:** الطباعة ثلاثية الأبعاد، أنابيب الكربون النانوية، طب الأسنان الرقمي، قاعدة الأسنان الصناعية، أنابيب الكربون النانوية.